Effects of Glycosylation on the Structure and Function of the Extracellular Chaperone Clusterin†

Elise M. Stewart,‡ J. Andrew Aquilina,‡ Simon B. Easterbrook-Smith,§ Danielle Murphy-Durland,‖ Christian Jacobsen,⊥ Soren Moestrup,⊥ and Mark R. Wilson*,‡

School of Biological Sciences and the Institute for Biomolecular Sciences, University of Wollongong, Northfields Avenue, Wollongong 2522, NSW, Australia, School of Molecular and Microbial Biosciences, University of Sydney, Sydney, Australia, Immunology and Inflammation Research Program, Garvan Institute of Medical Research, Sydney, Australia, and Institute of Medical Biochemistry, University of Aarhus, Denmark

Received October 5, 2006; Revised Manuscript Received November 13, 2006

ABSTRACT: Clusterin is the first well characterized, constitutively secreted extracellular chaperone that binds to exposed regions of hydrophobicity on non-native proteins. It may help control the folding state of extracellular proteins by targeting them for receptor-mediated endocytosis and intracellular lysosomal degradation. A notable feature of secreted clusterin is its heavy glycosylation. Although carbohydrate comprises approximately 20−25% of the total mass of the mature molecule, its function is unknown. Results from the current study demonstrate that deglycosylation of human serum clusterin had little effect on its overall secondary structure content but produced a small increase in solvent-exposed hydrophobicity and enhanced the propensity of the molecule to aggregate in solution. These changes were associated with increased binding to a variety of ligands but did not substantially impact the ability of clusterin to inhibit heat-induced precipitation of citrate synthase. Evidence suggesting that the normally conjugated sugars are important in the interaction of secreted clusterin with a lectin-type receptor on liver cells is also presented. Bulk expression of fully processed, glycosylated clusterin in mammalian cells is difficult, often producing inappropriately disulfide-bonded high molecular weight aggregates; this has hampered previous studies aimed at identifying those regions of the molecule important in its chaperone action. The current results suggest that it may be possible in the future to study the structure and chaperone function of clusterin using recombinant protein (lacking sugars) conveniently bulk-expressed in bacteria.

Clusterin is the first well characterized, constitutively secreted extracellular chaperone (EC) (*1*−*5*). We recently characterized another mammalian EC, haptoglobin (*6*). Clusterin and other ECs may help control the folding state of extracellular proteins by binding to exposed regions of hydrophobicity on non-native molecules to target them for receptor-mediated endocytosis and intracellular lysosomal degradation (*7*). In this way, they could protect the body from pathology arising from the inappropriate aggregation of damaged, partly unfolded extracellular proteins. Direct evidence for a role of clusterin in the *in vivo* clearance of aggregating proteins comes from the demonstration that aging clusterin knock-out mice develop progressive glomerulopathy characterized by the accumulation of insoluble protein (containing immunoglobulin) in the kidney (*8*). A protective role for clusterin is also supported by the observation that it behaves as an acute phase protein; clusterin expression is increased in a wide variety of models of stress and disease, including withdrawal of growth factors and exposure to noxious agents (*9*). Furthermore, the chaperone action of clusterin is enhanced under mildly acidic conditions, which occur *in vivo* during local acidosis found at sites of tissue damage or inflammation. The enhanced chaperone action at lower pH is thought to arise from an increased exposure to solvent of the hydrophobic regions on clusterin, concomitant with its increased dissociation from large oligomers into individual $\alpha-\beta$ heterodimers under these conditions (*4*).

A notable feature of secreted clusterin is its heavy glycosylation. Although carbohydrate comprises approximately 20−25% of the total mass of the mature molecule, its function is unknown. A total of six N-linked glycosylation sites have been identified, three in the alpha chain (α^{64}N, α^{81}N, and α^{123}N) and three in the beta chain (β^{64}N, β^{127}N, and β^{147}N). The types of oligosaccharides attached to the clusterin peptide are diverse (seven different possible types were identified on the basis of mass; (*10*)) and variable. The latter feature is thought to account for the observations that clusterin migrates in SDS−PAGE as a broad diffuse band and shows variable binding to Con A-Sepharose (*11*). During its chaperone action, clusterin binds to regions of exposed hydrophobicity on misfolded proteins to form solubilized high molecular weight complexes (*1*, *2*). One obvious but untested possibility is that the very hydrophilic carbohydrate

† E.M.S., M.R.W., and S.B.E. were supported by Discovery-Project Grants from the Australian Research Council (DP0211310 and DP0208752), and J.A.A. is supported by an Australian National Health and Medical Research Council R. D. Wright Career Development Award.

* Corresponding author. Tel: 61-242-214534. Fax: 61- 242-214135. E-mail: mrw@uow.edu.au.

‡ University of Wollongong.

§ University of Sydney.

‖ Garvan Institute of Medical Research.

⊥ University of Aarhus.

10.1021/bi062082v CCC: $37.00
Published on Web 01/09/2007

moieties might enhance the chaperone action of clusterin by helping it keep such complexes in solution. We developed a technique to enzymatically remove attached sugars from human serum-derived clusterin under native conditions and then performed a series of assays to compare the structure and *in vitro* function of wild type (WT[1]) and deglycosylated (DG) clusterin. We discovered that although deglycosylation of clusterin did not appear to induce major structural changes, it did increase the amount of solvent-exposed hydrophobicity, the tendency of the molecule to aggregate in solution, and its binding to a range of ligands. Surprisingly, deglycosylation did not substantively impact the ability of clusterin to inhibit the heat-induced precipitation of citrate synthase (a model chaperone substrate).

MATERIALS AND METHODS

Materials. 4,4′-Bis(1-anilino-8-naphthalene sulfonate) (bisANS), bovine serum albumin (BSA), citrate synthase (CS), galactose, iodoacetamide (IAA), lysozyme, *o*-phenylenediamine dihydrochloride (OPD), propidium iodide (PI), and superoxide dismutase were all obtained from Sigma (St. Louis, MO). Dithiothreitol (DTT) was obtained from Boehringer Mannheim (Sydney, Australia). *N*-(2-hydroxyethyl)piperazine-*N*′-(2-ethanesulfonic acid) (HEPES) was obtained from USB (OH). All buffer salts and H_2O_2 were obtained from Ajax Chemical Co. (Sydney, Australia). Human blood was obtained as a kind gift from Wollongong Hospital (Wollongong, NSW, Australia) and processed to yield plasma, which was stored frozen at −20 °C until use. Clusterin was purified from human plasma by immunoaffinity chromatography as previously described (*12*). *N*-glycosidase F was obtained from Roche (Sydney, Australia). Glutathione-*S*-transferase (GST) was prepared by thrombin cleavage of GST-fusion proteins as described (*13*). IgG was purified from human plasma using a HiTrap protein G cartridge fitted to an Akta Explorer chromatography system (G E Healthcare, Sydney, Australia). The hybridoma cell line secreting the $IgG_1\kappa$ anti-clusterin MAb G7 was a gift from Dr. B. Murphy (St. Vincent's Hospital, Melbourne, Australia). 78E and 41D, $IgG_1\kappa$ anti-clusterin MAbs, and DNP-9, an $IgG_1\kappa$ MAb that binds specifically to the 2,4-dinitrophenyl group, have been described previously (*14*, *15*).

Enzymatic Deglycosylation of Clusterin. For large scale digestions, *N*-glycosidase F (400 U; about 16 μg) was added to 4 mg of purified WT clusterin in 4 mL in phosphate buffered saline (PBS; 137 mM NaCl, 2.7 mM KCl, 1.5 mM KH_2PO_4, and 8 mM Na_2HPO_4 at pH 7.4) and incubated at room temperature for 6−12 h with gentle agitation. Deglycosylation was confirmed by SDS−PAGE and mass spectrometry analyses.

Mass Spectrometry. Deglycosylated (DG) clusterin in PBS was reduced with 5 mM DTT for 15 min at room temperature prior to acidification with 99% formic acid to a final concentration of 10% (v/v). A ZipTip (Millipore) was used to remove nonvolatile salts by washing the C_{18} bound protein with 1% aqueous formic acid, followed by elution in 3 μL of 72% acetonitrile/10% formic acid directly into a gold-coated borosilicate nanoelectrospray (nanoESI) capillary (prepared in-house). Spectra were acquired on an Ultima hybrid quadrupole time-of-flight mass spectrometer (Micromass UK, Ltd.) and calibrated using a horse heart myoglobin spectrum acquired on the same day. Selected conditions were as follows: capillary voltage, 1.5 kV; cone gas, 150 Lh^{-1}; sample cone, 200 V; RF lens 1 energy, 100 V; source and desolvation temperature of 20 °C; and base pressures throughout. Spectra were acquired over the range *m*/*z* 600 to *m*/*z* 5000, and the resultant data were transformed, after minimal smoothing, to a mass scale using an algorithm in the MassLynx software (Waters/Micromass).

Circular Dichroism Spectrometry. A Jasco Model J-810 (Jasco, Canada) spectropolarimeter linked to a CDF-426S/L Peltier system (Jasco, Canada) was used to acquire circular dichroism (CD) data. Far-UV (190−250 nm) CD studies were performed using a 1.0 mm path length cell with WT and DG clusterin, each at 1.6 μM in 10 mM sodium phosphate, pH 7.5 or pH 6 at 25 °C. Spectra were acquired at 100 millidegree sensitivity with a step resolution of 0.1 nm and a bandwidth of 1.0 nm. The raw data were corrected for the buffer signal and mean residue ellipticity (θ_{MRE}) values then calculated from them assuming that both WT and DG clusterin contain 427 residues, that DG clusterin has a calculated molecular mass of 50 kDa, and that WT clusterin has an average molecular mass of 61 kDa (*10*). Estimates of the percentages of α-helical, β-sheet, β-turn, and unordered secondary structure were then made by deconvolution of the θ_{MRE} data using the programs CDSSTR, SELCON (*16*), and CONTIN-LL (*17*). The deconvolution data reported are means ± standard deviations of the estimates made by these three programs.

Measurements of BisANS Fluorescence. The fluorescence of bisANS bound to WT and DG clusterin was measured using a FLUOstar OPTIMA microplate reader (BMG Labtech, Melbourne, Australia). Samples of clusterin (0.66 μM in 10 mM Na_2HPO_4, 10 mM MES, 150 mM NaCl at pH 6.0 or pH 7.5; 50 μL/well) were added to a black 96-well plate (Costar 3915; Crown Scientific, Sydney). An equal volume of bisANS in the same buffers was added to wells containing clusterin (at the corresponding pH) to give various final concentrations up to 20 μM. The plate was then incubated at 28 °C for 15 min before measuring the fluorescence of the samples at 490 ± 5 nm with excitation at 360 ± 5 nm. The data shown have been corrected for the fluorescence of control samples containing only bisANS.

Equation 1, which describes the binding of bisANS to a single class of binding sites on clusterin, was fitted to the data by nonlinear regression analysis using SigmaPlot v8.02 (SPSS, Chicago, IL).

$$F = F\text{max.}[\text{bisANS}]/(K\text{d} + [\text{bisANS}]) \qquad (1)$$

In this equation, F, Fmax, and K_d are the observed fluorescence, the fluorescence at saturating concentrations of bisANS and the apparent dissociation constant, respectively.

Size Exclusion Chromatography. A 22 mL bed volume (1.0 × 30 cm) Superose-6 column (GE Healthcare, Sydney) was equilibrated with 100 mM sodium phosphate and 100

[1] Abbreviations: bisANS, 4,4′-bis(1-anilino-8-naphthalene sulfonate); BSA, bovine serum albumin; CS, citrate synthase; DG, deglycosylated; DTT, dithiothreitol; IAA, iodoacetamide; GST, glutathione-*S*-transferase; HDC, heat-denatured casein; IgG, immunoglobulin G; lys, lysozyme; OPD, *o*-phenylenediamine dihydrochloride; PBS, phosphate buffered saline; PI, propidium iodide; WT, wild type.

mM NaCl, containing 0.05% sodium azide at pH 6.0 or pH 7.5 at room temperature before samples were loaded at 2.6 μM (heterodimer) in 100 μL of equilibration buffer. Protein was passed over the column at a flow rate of 0.5 mL/min and the absorbance at 280 nm of the eluate continuously quantified using an AKTA FPLC (GE Healthcare, Sydney). Mass standards from both Low and High Molecular Weight Gel Filtration kits were analyzed following the manufacturer's instructions (GE Healthcare, Sydney).

ELISA. The binding of WT and DG clusterin to known native protein ligands (*18*) and protein ligands "stressed" by either heat or reduction (*1*) was tested in ELISA.

Native Protein Ligands. 96-Well ELISA plates (Greiner, Germany) were coated with human IgG (*12*) or GST (*1*) (both at 10 μg/mL in PBS) before blocking wells with 1% (w/v) heat-denatured casein in PBS (HDC/PBS). All coating, blocking, and binding steps were performed for 1 h at 37 °C. WT or DG clusterin at various concentrations, diluted in HDC/PBS, were then incubated in the wells. To minimize nonspecific binding of clusterin to the ELISA plates, three washes were then performed with 0.1% (v/v) Triton X-100 in PBS. A cocktail of tissue culture supernatants containing G7, 78E, and 41D anti-clusterin monoclonal antibodies was used to detect bound clusterin, and DNP-9 culture supernatant was used as an isotype control. Independent ELISA experiments demonstrated that this antibody cocktail detected WT and DG clusterin with equal efficiency (data not shown). Bound primary antibodies were detected with sheep-anti-mouse-Ig-HRP (Silenus, Sydney, Australia), using *o*-phenylenediamine dihydrochloride (OPD; 2.5 mg/mL in 0.05 M citric acid and 0.1 M Na_2HPO_4 at pH 5.0, containing 0.03% (v/v) H_2O_2) as substrate and measuring the final absorbance at 490 nm with a SpectraMax Plus^{384} microplate reader (Molecular Devices, USA). Nonspecific binding was assessed by measuring the binding to wells coated with only HDC/PBS.

Stressed Protein Ligands. BSA (1 mg/mL in PBS ± 20 mM DTT) was coated onto ELISA plates during a 16 h incubation at 4 °C. In order to exclude the possibility of subsequent formation of disulfide bonds between reduced BSA and clusterin, DTT-treated wells were then incubated with 5 mM IAA in PBS (to block any free sulfydryl groups; (*1*)). The wells were subsequently blocked with 1% (w/v) BSA in PBS. In other experiments, the wells were coated for 16 h with lysozyme (0.25 mg/mL in PBS) at either 43 or 4 °C before blocking with HDC/PBS. For these two types of ELISA, nonspecific binding of clusterin was assessed using wells coated with BSA in the absence of DTT, or coated with lysozyme at 4 °C, respectively; other procedures in these assays were as described above. Equation 2, which describes the binding of clusterin to a single class of binding sites on the protein ligands, was fitted to the ELISA data by nonlinear regression analysis as described above.

$$A = A\text{max.}[\text{clusterin}]/(K\text{d} + [\text{clusterin}]) \qquad (2)$$

In this equation, A, Amax, and K_d are the observed absorbance, the absorbance at saturating concentrations of clusterin, and the apparent dissociation constant, respectively.

Protein Precipitation Assays. Citrate synthase (CS; 2 μM), with or without WT or DG clusterin (at 1.3 or 3.9 μM), in phosphate buffer (100 mM sodium phosphate and 100 mM NaCl, containing 0.05% sodium azide at pH 6.0 or pH 7.5) was heated at 43 °C for 100−250 min in 384-well plates (100 μL/well) in a SpectraMax Plus^{384} microplate reader (Molecular Devices, USA). Protein precipitation was measured as turbidity (absorbance at 360 nm; A^{360}). To confirm that the effects of clusterin were specific, in some experiments, superoxide dismutase was used as a control protein.

Surface Plasmon Resonance (SPR) Analysis. The binding to megalin was studied by SPR analysis on a Biacore 3000 instrument (Biacore, Sweden). The procedure was as follows. Biacore sensor chips type CM5 were activated with a 1:1 mixture of 0.2 M *N*-ethyl-*N*′-(3-dimethylaminopropyl)carbodiimide and 0.05 M *N*-hydroxysuccimide in water according the manufacturer. Rabbit megalin (purified as described previously (*19*)) was immobilized at a concentration of 10 μg/mL in 10 mM sodium acetate at pH 4.5. The remaining binding sites were blocked with 1 M ethanolamine at pH 8.5. A control flow cell was made by only performing the activation and blocking procedure. The surface plasmon resonance signal from immobilized megalin generated 17,-588 Biacore response units equivalent to a resulting receptor density of 24 fmol megalin/mm^2. Samples were dissolved in 10 mM Hepes, 150 mM NaCl, 3.0 mM $CaCl_2$, and 1 mM EGTA at pH 7.4 + 0.005% Tween 20. The sample and running buffer were identical. Regeneration of the sensor chip after each analysis cycle was performed with 1.6 M glycine-HCl buffer at pH 3.0. The Biacore response is expressed in relative response units (RU), that is, the difference in response between protein and control flow channels. Kinetic parameters were determined by BIAevaluation 4.1 software using a Langmuir 1:1 binding model and simultaneous fitting of all curves in the concentration range (global fitting).

Cell Culture and Flow Cytometry. HepG2 (human hepatocarcinoma) cells (ATCC, MA) were cultured in DMEM/F12 medium containing 5% (v/v) fetal bovine serum (Trace Biosciences, Melbourne, Australia) at 37 °C and 5% (v/v) CO_2. For binding experiments, cells were grown to confluency and removed from the plastic surface by incubating for 5−10 min with PBS containing 5 mM EDTA. Cells were then washed by centrifugation (5 min at 300 g) with Hank's buffered saline (HBS; 137 mM NaCl, 20 mM HEPES, 5.4 mM KCl, 0.25 mM Na_2HPO_4, 0.44 mM KH_2PO_4, 1.3 mM $CaCl_2$, and 1.0 mM $MgSO_4$ at pH 7.4). Cell pellets were resuspended and incubated on ice for 30 min in 100 μL of HBS containing 10 mg/mL BSA (BSA/HBS) and either no additions or 2 μM clusterin (WT or DG) with or without 5 mM galactose. Bound clusterin was detected by next incubating washed cells in a cocktail of tissue culture supernatants containing G7, 78E, and 41D anti-clusterin monoclonal antibodies, diluted 1 in 2 in BSA/HBS; DNP-9 culture supernatant was used as an isotype control. Finally, after washing with HBS, cell pellets were next suspended and incubated for 30 min on ice in 100 μL of sheep-anti-mouse immunoglobulin-FITC conjugate. An LSR II flow cytometer (Becton Dickinson, Sydney, Australia) was used to analyze cells that were incubated with 1 μg/mL PI immediately before analysis to stain the nuclei of dead cells. Cells were excited at 488 nm and fluorescence emissions collected at 515 ± 10 nm (FITC) and 695 ± 20 nm (PI). Electronic gating was used to exclude dead cells from the analyses. Data was collected using FACS Diva software

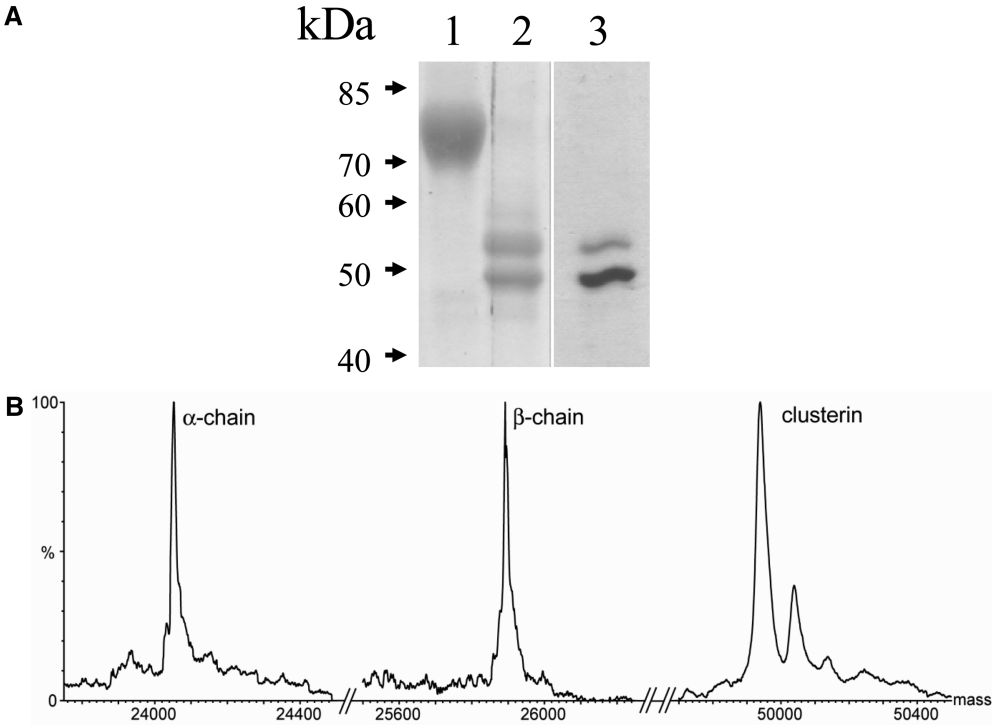

FIGURE 1: Enzymatic deglycosylation of human serum clusterin. (A) Composite image of two Coomassie blue-stained SDS−PAGE gels showing WT clusterin (lane 1) and DG clusterin (lanes 2 and 3). Lane 2 shows 10 μg of protein removed from a reaction mixture comprising 4 mL of PBS, containing 4 mg of WT clusterin and 200 U of *N*-glycosidase, which had been incubated at room temperature for 6 h. Lane 3 shows 10 μg of protein removed from the same reaction mixture after adding a further 100 U of *N*-glycosidase F and an additional 6 h of incubation at room temperature. (B) Transformed mass spectrum of DG clusterin following reduction and acidification. The peaks at 24,197 and 25,883 Da arise from the α- and β-chains of clusterin, respectively. Although the protein was subject to harsh denaturing conditions, a proportion of intact clusterin was observed, as evidenced by the peak at 49,943 Da. The minor peak at 50,041 Da corresponds to the faint upper band visible in lane 3 in (A), a species with a small amount of residual glycosylation. Breaks in the *x*-axis have been used to accommodate all peaks within one spectrum.

(v4.0; Becton Dickinson) and analyzed using FloJo v6.4.1 (Treestar Inc., USA).

RESULTS

Enzymatic Deglycosylation of Human Clusterin. Prolonged treatment of human serum clusterin with *N*-glycosidase F under native conditions was shown to be sufficient to remove the vast majority of attached sugars from the polypeptide backbone (Figure 1). When 4 mg of WT clusterin was exposed to 200 U of *N*-glycosidase F for 6 h at room temperature and then analyzed by SDS−PAGE, the pattern of migration of the protein changed from a diffuse band at 75−80 kDa to a doublet of narrower bands centered at just above 50 kDa (compare lanes 1 and 2 in Figure 1A). Further incubation with additional *N*-glycosidase F reduced the intensity of the upper band in the doublet (lane 3, Figure 1A). The predicted molecular mass of the clusterin polypeptide is 50,080 Da (Swiss-Prot entry P10909). Thus, the SDS−PAGE estimate of the mass of the principal species present at the end of the digestion (the lower band in lane 3, Figure 1A) is in good agreement with the theoretical mass of fully deglycosylated human clusterin (DG clusterin).

Mass Spectrometry Analysis of DG Clusterin. Because of the high level of clusterin glycosylation, data concerning the mass of the protein chains has previously been confined to translation of the nucleotide sequence and very low-resolution MALDI mass spectra (*10*). Preparation of DG clusterin in this study has enabled us to examine the masses of the α- and β-chains as well as intact clusterin with unprecedented accuracy. For simplicity, the raw mass spectral data were processed and transformed to a mass scale. Figure 1B shows the mass peaks attributed to the individual α- and β-chains and intact clusterin. Predicted masses for these species based on sequence data from Swiss-Prot entry P10909 are 24,197, 25,883, and 50,080 Da, respectively. The action of *N*-glycosidase F converts asparagine-bound *N*-glycans to aspartic acid residues with a concomitant increase in mass of 1 Da per residue (*20*). There are 3 Asn residues linked to glycans on each of the α and β chains of clusterin (*10*); thus, the action of the enzyme would increase the predicted mass of each subunit chain by 3 to 24,200 and 25,886 Da, respectively. Clearly, there is a major discrepancy between the predicted and observed masses (24,051 ± 1 Da) for the α-chain, which in turn affected the observed mass of intact clusterin. The β-chain, at 25,895 ± 2 Da, however, was only 9 Da higher than the theoretical mass. Although the protein was subject to harsh denaturing conditions, a proportion of intact clusterin was detected as a peak at 49,943 Da. A minor peak at 50,041 Da was consistent with the presence of a faint band detected by SDS−PAGE electrophoresis, which migrated a lesser distance than the major species of DG clusterin (Figure 1A). The relatively large separation observed between the two bands in Figure 1A (lanes 2 and 3) cannot be explained by the 98 Da difference in mass determined by MS but very probably results from the well-known anomalous migration of glycoproteins frequently observed in SDS−PAGE (*21*). This is illustrated also by WT (fully glycosylated) clusterin, which migrates in SDS−PAGE

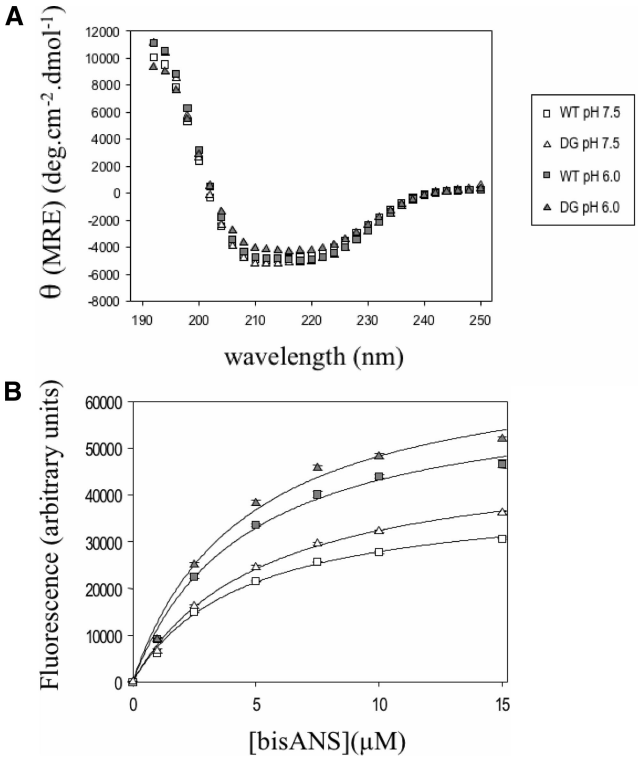

FIGURE 2: (A) Far-UV CD for WT and DG clusterin at pH 6.0 and 7.5 (see key); the mean residue ellipticity (θ) is plotted against wavelength. Data were acquired at 0.5 nm intervals but are plotted at 2 nm intervals for clarity. The data shown are the means of six scans. (B) BisANS fluorescence (in arbitrary units) of WT and DG clusterin over a range of concentrations from 0 to 15 μM. The data points shown represent the means of triplicate determinations, and the error bars are standard errors of the means. The result shown is representative of several independent experiments. The curves drawn are lines of best fit of eq 1 (Materials and Methods). The key shown in (A) also applies here.

Table 1: Predicted Percentages (± Standard Errors) of Secondary Structural Features for WT and DG Clusterin at pH 6.0 and 7.5, Based on Far-UV CD Data.

protein (pH)	α-helix (%)	β-sheet (%)	β-turn (%)	unordered (%)
WT clusterin (7.5)	43.2 ± 1.7	16.0 ± 1.1	14.0 ± 1.0	26.5 ± 2.1
DG clusterin (7.5)	39.8 ± 3.1	17.4 ± 1.3	15.5 ± 0.8	27.7 ± 1.7
WT clusterin (6.0)	43.3 ± 1.8	15.9 ± 1.0	14.1 ± 0.9	26.7 ± 1.6
DG clusterin (6.0)	37.1 ± 1.9	18.4 ± 1.4	16.5 ± 0.3	27.9 ± 2.1

with an apparent mass of 75−80 kDa (Figure 1A, lane 1) but which actually has a mass of about 61 kDa, determined by MS (*10*).

CD Analyses of WT and DG Clusterin. In order to assess the effects of deglycosylation of clusterin on its overall secondary structure, samples of WT and DG clusterin were analyzed by far-UV CD at pH 7.5 and 6.0. The CD spectra obtained (Figure 2A) were similar; their local minima at ∼222 nm and ∼208 nm suggest that both WT and DG clusterin contain substantial amounts of α-helix. Deconvolution of these spectra using the programs CDSSTR, SELCON, and CONTIN-LL gave the predicted secondary structural percentages shown in Table 1. The finding that there was no significant difference in the predicted secondary structure of WT clusterin at pH 6 compared to that at pH 7.5 corroborates our previous results (*22*). Moreover, the finding that the predicted overall secondary structure of DG clusterin was not significantly different to that of WT clusterin at either pH 7.5 or at pH 6.0 suggests that deglycosylation of clusterin does not lead to gross changes in its secondary structure.

Table 2: Estimated Values (± Standard Errors, SE) of Binding Affinity (K_d) and Maximum Fluorescence (*F*max; in Arbitrary Fluorescence Units, AFU) for the Binding of BisANS to WT and DG Clusterin.

protein form	pH	*K*d ± SE (μ**M**)	*F*max ± SE (AFU)
WT	7.5	4.4 ± 0.4	40170 ± 1353
	6	4.5 ± 0.6	62560 ± 2909
DG	7.5	5.2 ± 0.4	49270 ± 1592
	6	4.5 ± 0.8	70030 ± 4566

BisANS Fluorescence Analyses. At pH 7.5, the pattern of dose-dependent bisANS fluorescence was very similar for WT and DG clusterin (Figure 2B). The estimates of K_d for the binding of bisANS to each species are, within experimental error, the same (Table 2). Under these conditions, the maximum bisANS fluorescence (*F*max) estimated for DG clusterin was significantly greater (by about 20%; student's *t*-test, $p < 0.001$) than that measured for WT clusterin (Table 2). The estimates of K_d for the binding of bisANS to WT and DG clusterin at pH 6.0 are not significantly different to those for pH 7.5. However, the estimates of *F*max for both WT and DG clusterin are significantly higher (by about 40−55%; student's *t*-test, $p < 0.001$) than the corresponding values for pH 7.5 (Figure 2B, Table 2). Taken together, these data imply that at pH 7.5, DG clusterin exposes slightly greater hydrophobicity to solution than WT clusterin and that under the conditions tested, pH 6.0 induces a significant increase in exposed hydrophobicity on both DG and WT clusterin.

Size Exclusion Chromatography. Clusterin exists in aqueous solution as a mixture of oligomers of widely ranging mass (*1*). It shares this property of polydispersity in solution with a range of other chaperones, including members of the small heat shock protein family (*23*). When analyzed by size exclusion chromatography, at pH 7.5 WT clusterin migrated as a mixture of species, including a small fraction at the exclusion limit of the column (>2000 kDa), a major peak at about 400 kDa, and some presumptive $\alpha-\beta$ monomer at about 80 kDa (Figure 3, upper panel). At pH 6.0, this pattern was similar except that the proportion of species in lower order aggregation states was increased (as expected (*4*)), most obviously at about 80 kDa (representing individual $\alpha-\beta$ heterodimers; Figure 3, lower panel). Compared with WT clusterin, at pH 7.5, DG clusterin species were biased toward larger oligomers, with a major peak centered at about 900 kDa and little apparent monomers (Figure 3, upper panel). At pH 6.0, again there was a shift toward lower order aggregates, with major peaks at about 400 and 150−160 kDa and a small monomer peak at about 50 kDa (indicated by the arrow in Figure 3, lower panel). Relative to WT clusterin, a greater proportion of DG clusterin species remained as large aggregates at pH 6.0; this was particularly apparent at an elution volume of 10.5−11.0 mL (i.e., about 1600 kDa) where DG clusterin, but not WT clusterin, maintained a major oligomer peak.

Binding to Native and Stressed Protein Ligands. Both WT and DG clusterin showed enhanced binding to all ligands

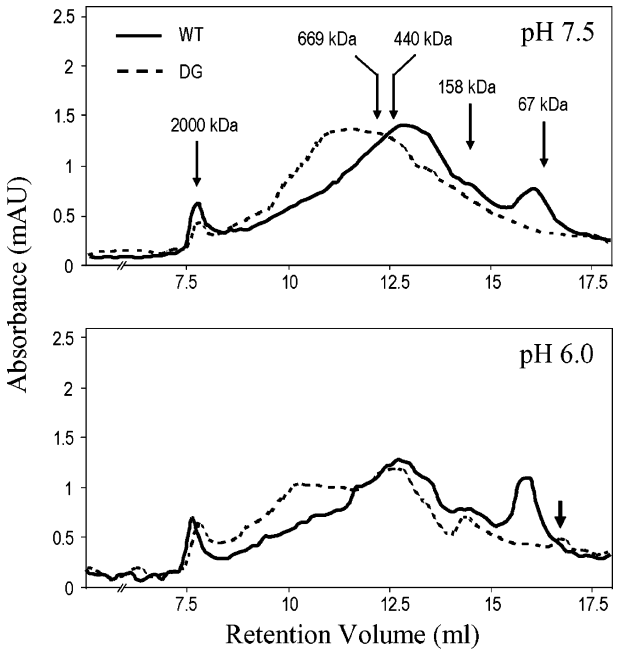

FIGURE 3: Absorbance traces (280 nm) for size exclusion chromatographic analyses of individual solutions of WT clusterin (—) and DG clusterin (---) at pH 7.5 and pH 6.0 (indicated on plots). Positions of molecular mass markers are indicated by labeled arrows on the upper panel; these were dextran blue (2000 kDa, 7.9 mL), thyroglobulin (669 kDa, 12.5 mL), ferritin (440 kDa, 12.7 mL), aldolase (158 kDa, 14.5 mL), and albumin (67 kDa, 16.5 mL). The position of a small peak at about 50 kDa (putative DG clusterin monomer) is indicated by the arrow on the lower panel. The results shown are representative of two independent experiments.

tested at pH 6.0 versus pH 7.5 (Figure 4A−D). This behavior has been described before for WT clusterin binding to reductively stressed BSA (*4*). For IgG, both WT and DG clusterin bound with higher affinity at pH 6.0 than at pH 7.5. Relative to WT, DG clusterin bound to a higher level to IgG at both pH values and with greater affinity at pH 6.0 (Table 3). In Figure 4A, the maximum absorbance (*A*max) values for WT and DG clusterin cannot be directly compared between pH 6.0 and pH 7.5 because these results were obtained from independent experiments performed on different ELISA trays. However, in other experiments, it was found that changing the pH from 7.5 to 6.0 did not significantly affect *A*max for either WT or DG clusterin (data not shown). In contrast, there were only very minor differences between WT and DG clusterin with respect to their binding to GST; both showed increased affinity at lower pH (Figure 4B; Table 3). In the case of heat-stressed lysozyme, the lower pH increased both the affinity and maximum binding of WT and DG clusterin (Figure 4C). The maximum binding and affinity of DG clusterin for heat-stressed lysozyme was greater than that for WT clusterin at both pH values (Table 3). Finally, for reductively stressed BSA, the affinity and maximum binding of WT clusterin was greater at pH 6.0 than at pH 7.5. In contrast, DG clusterin bound very strongly at pH 7.5 and showed only a small increase in binding at pH 6.0; the affinity of DG clusterin binding was very similar at both pH values (Table 3).

SPR Analysis of Binding to Megalin. SPR measurements of the binding of WT and DG clusterin, at various concentrations, to immobilized megalin are shown in Figure 5. These data show very similar estimates of the overall binding affinity (K_d) for the two species; however, the association (k_a) and dissociation (k_d) constants for DG clusterin are more than four times greater than those of WT clusterin (Table 4), indicating that the removal of sugars from clusterin increased the rate at which it bound to and dissociated from megalin.

In Vitro Chaperone Action. At either pH tested, when present at a slight molar excess (molar ratio of clusterin/CS = 1.95:1.0), both WT and DG clusterin gave near-complete inhibition of CS precipitation over the time course studied (Figure 6). Inhibition of CS precipitation was partial at lower concentrations of clusterin (clusterin/CS = 0.65:1.0). Under these latter conditions, WT clusterin inhibited CS precipitation more effectively at pH 6.0 than at pH 7.5, consistent with the known enhancement of WT clusterin chaperone action at mildly acidic pH (*4*). DG clusterin was slightly more effective than WT clusterin at inhibiting CS precipitation at pH 7.5 (Figure 6, upper panel) but at pH 6.0 did not show a significant change in chaperone activity; at the lower pH, both WT and DG clusterin inhibited CS precipitation to a comparable extent (Figure 6, lower panel).

Binding to HepG2 Cells. There was little difference in the overall binding affinities of WT and DG clusterin for megalin (Figure 5 and Table 4). However, recent studies have suggested that clusterin may also bind to a variety of other cell surface receptors (*24*). Considering the possibility that clusterin might be bound by lectin-type receptors via their attached sugars, we compared the binding of WT and DG clusterin to cultured HepG2 (human hepatocarcinoma) cells and tested whether the binding of either could be inhibited with monomeric sugars. The total binding of WT clusterin to HepG2 cells was greater than that of DG clusterin (compare the thick lines on the two panels shown in Figure 7). Furthermore, the binding of WT clusterin was significantly inhibited by co-incubation with 5 mM galactose, whereas this treatment had little effect on the binding of DG clusterin (compare thin vs thick lines on both panels of Figure 7).

DISCUSSION

We report here for the first time conditions suitable for the near-complete enzymatic removal of sugars from human serum clusterin under native conditions. The success of this procedure was verified by SDS−PAGE and MS analyses (Figure 1). The discrepancy in mass for the β-chain may be due to a sequence conflict such as Q47H as reported by de Silva et al. (*25*) for the α-chain (the numbering used here refers to the full-length precursor protein). However, the lower observed mass for the α-chain suggests either multiple residue variations from those predicted by the nucleotide sequence or, more likely, a residue deletion following processing of the full length precursor to the disulfide-linked chains. The C-terminal residue of the α-chain is reported to be an Arg at position 227 (*26*). Previous peptide mass analyses indicated the presence of Arg227 at the C-terminus of clusterin immunoaffinity purified from freshly obtained human plasma, which had been supplemented with protease inhibitors within 15 min of venepuncture (*10*). In the current study, blood was obtained from a hospital usually within 1−2 h of venepuncture; the additional time between venepunc-

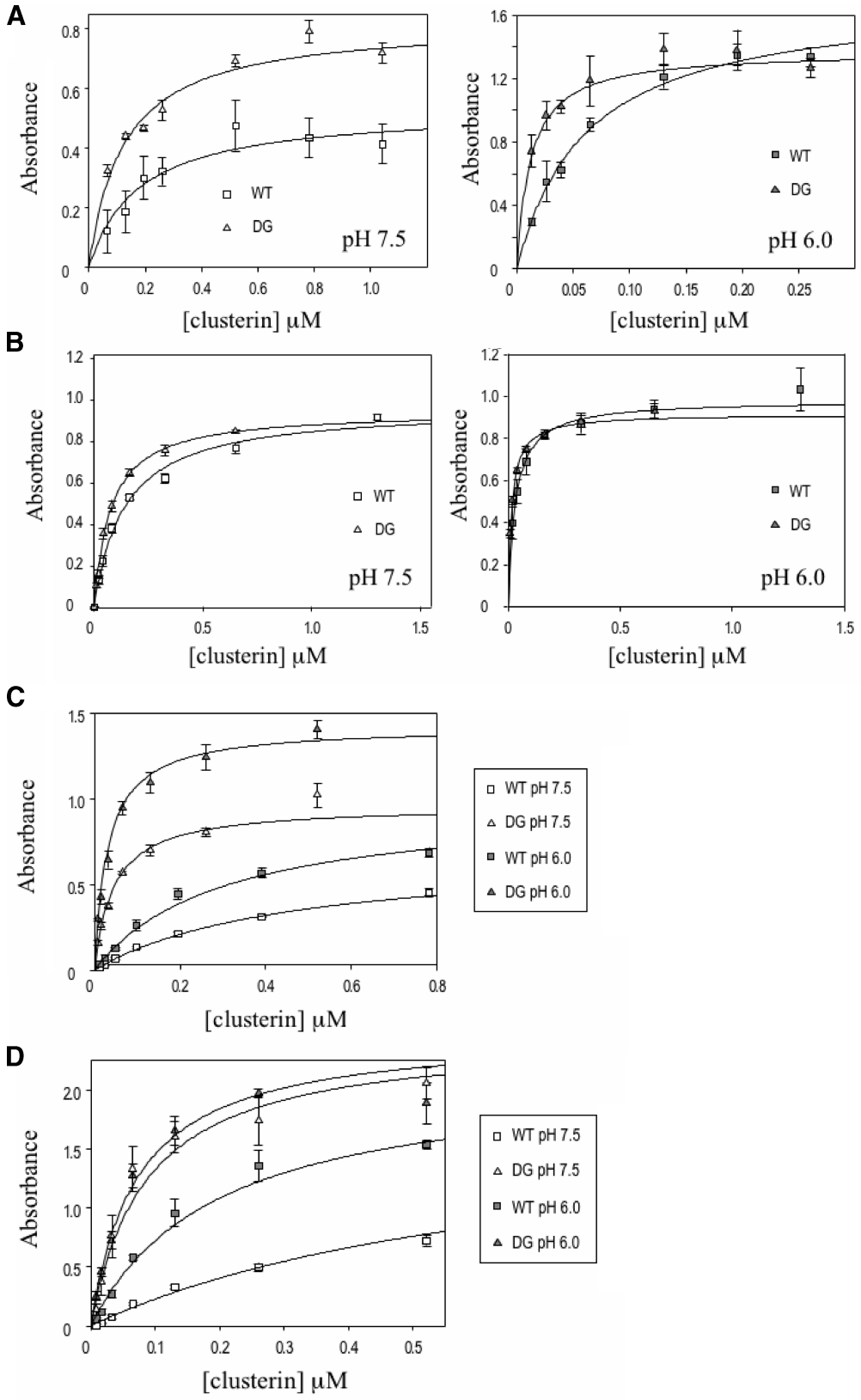

FIGURE 4: Results of ligand binding ELISAs. The binding of WT and DG clusterin to (A) human IgG, (B) GST, (C) heat-stressed lysozyme, and (D) reductively stressed BSA, at pH 7.5 and 6.0 (see keys in or near respective panels). Each data point represents the mean of triplicate determinations, and the error bars are standard errors of the mean in each case. The data shown are representative of several independent experiments. Estimated kinetic parameters for these data are shown in Table 3.

ture and the addition of protease inhibitors may have allowed sufficient time for the proteolytic removal of Arg227 from the C-terminus of the clusterin α-chain. A candidate protease potentially responsible for this is carboxypeptidase N, a plasma zinc metalloprotease that cleaves basic amino acids, lysine and arginine, from the carboxy terminus of proteins (*27*). This cleavage would result in a loss of 156 Da for the α-chain to yield a theoretical mass of 24,044 Da. The above-

Table 3: Analysis of the Binding of WT and DG Clusterin to Stressed Proteins in ELISA[a]

	WT clusterin		DG clusterin		statistical significance		
target	*A*max ± SE	*K*d ± SE (*μ*M)	*A*max ± SE	*K*d ± SE (*μ*M)	pH	DG/WT pH 6.0	DG/WT pH 7.5
			IgG				
pH 6.0	1.71 ± 0.07	0.059 ± 0.007	1.42 ± 0.05	0.013 ± 0.002	WT; K_d, N/A	K_d, *A*max	*A*max
pH 7.5	0.54 ± 0.06	0.18 ± 0.06	0.85 ± 0.05	0.13 ± 0.03	DG; K_d, N/A		
			GST				
pH 6.0	1.0 ± 0.04	0.03 ± 0.01	0.93 ± 0.01	0.035 ± 0.002	WT; K_d	neither	neither
pH 7.5	0.97 ± 0.04	0.14 ± 0.02	0.95 ± 0.02	0.15 ± 0.01	DG; K_d		
			lysozyme				
pH 6.0	0.90 ± 0.06	0.23 ± 0.05	1.47 ± 0.04	0.039 ± 0.003	WT; K_d, *A*max	K_d, *A*max	K_d, *A*max
pH 7.5	0.72 ± 0.03	0.48 ± 0.04	1.07 ± 0.05	0.06 ± 0.01	DG; K_d, *A*max		
			BSA				
pH 6.0	2.12 ± 0.15	0.17 ± 0.03	2.29 ± 0.12	0.06 ± 0.01	WT; K_d, *A*max	K_d	K_d, *A*max
pH 7.5	1.29 ± 0.11	0.41 ± 0.06	2.28 ± 0.14	0.06 ± 0.02	DG; neither		

[a] The estimates (± standard errors, SE) for maximum absorbance (*A*max) and the binding affinity (*K*d) were obtained by nonlinear regression of eq 2 onto the data shown in Figure 4, as described in Materials and Methods. The statistical significance of differences between these estimates was assessed by student's *t*-test; values of *t* giving $p < 0.05$ were considered significant. Entries in the pH column refer to comparisons of the effects of pH on *K*d and *A*max for each protein, whereas entries in the DG/WT pH 6.0 and DG/WT pH 7.5 columns refer to comparisons between *K*d and *A*max for each protein at the indicated pH values. N/A indicates that for IgG, the data shown were acquired from independent experiments at pH 6.0 and 7.5; it is, therefore, meaningless to compare these *A*max values.

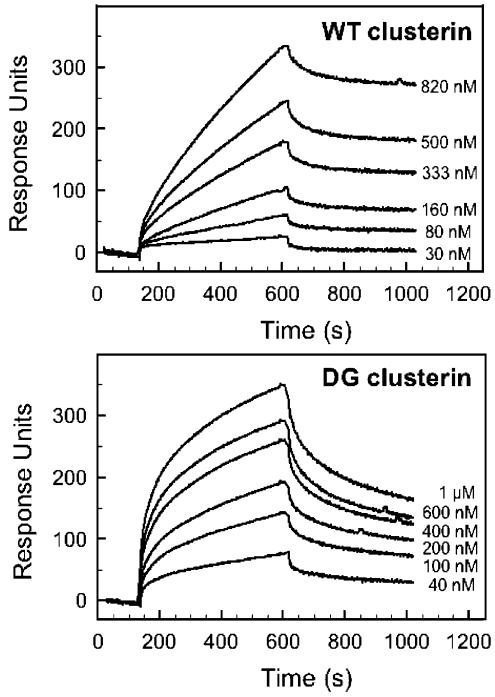

FIGURE 5: Surface plasmon resonance analysis of clusterin binding to megalin. Megalin was immobilized onto sensor chips, and samples of WT clusterin and DG clusterin (40 μL) were injected over the flow cells at 5 μL/min. The sensorgrams were recorded at the indicated concentrations for evaluation of kinetic parameters. Kinetic parameters estimated from these data are shown in Table 4.

Table 4: Estimated Kinetic Constants for the Binding of WT and DG Clusterin to Megalin[a]

form of clusterin	mol. wt. (kDa)	K_d (nM)	k_a ($M^{-1}s^{-1}$)	k_d (s^{-1})
WT	61	~150	1.7×10^3	2.5×10^{-4}
DG	50	~140	8.0×10^3	1.1×10^{-3}

[a] The overall binding affinity (K_d) and the association and dissociation constants (k_a and k_d, respectively) are shown.

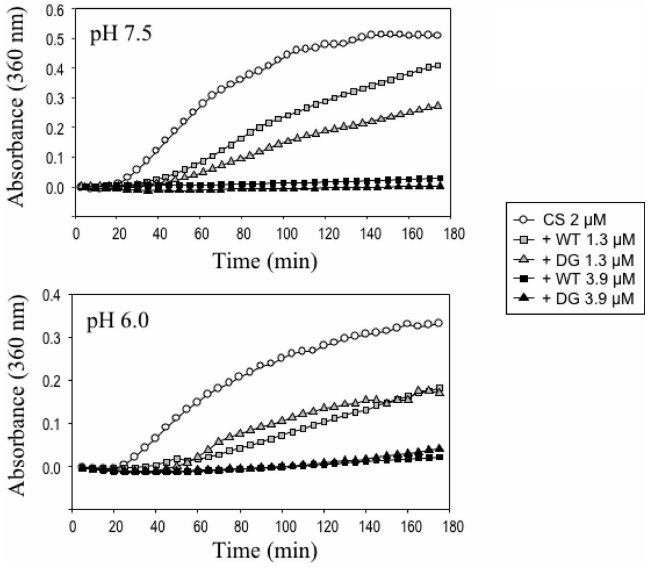

FIGURE 6: Plots showing time-dependent changes in turbidity (measured as absorbance at 360 nm) of 2 μM solutions of CS (at pH 7.5 or pH 6.0, indicated) heated at 43 °C with either no additions or containing WT or DG clusterin at 1.3 or 3.9 mM (see key). The data points shown represent individual measurements. The results shown are representative of several independent experiments.

reported Q47H sequence conflict would, within the reported mass error, account for the remaining 7 Da difference.

The effects of enzymatic deglycosylation on clusterin structure were investigated using CD, bisANS fluorescence, and size exclusion chromatographic analyses. Owing to the known effect of mildly acidic pH on clusterin structure and function (*4*), these analyses were performed at both pH 6.0 and 7.5. Far-UV CD measurements indicated that at either pH, the spectra and predicted percentages of secondary structures of WT and DG clusterin were very similar (Figure 2A, Table 1), suggesting that deglycosylation of clusterin did not bring about any gross changes in its secondary structure. Deglycosylation did slightly increase the *F*max for the binding of bisANS to clusterin at pH 6.0 and 7.5 (Figure 2B, Table 2), suggesting that the removal of sugars marginally increased the area of solvent-exposed regions of

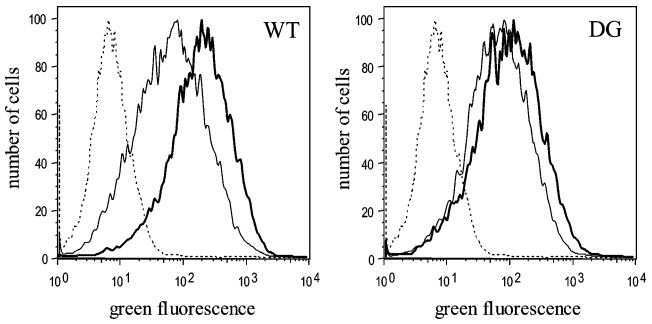

FIGURE 7: Flow cytometry overlay histograms of fluorescence, representing the binding of WT (left panel) and DG (right panel) clusterin to the surface of HepG2 cells. Treatments are 2 μM clusterin alone (thick line) or in the presence of 5 mM galactose (thin line). The dotted line represents cells incubated with 2 μM clusterin but subsequently incubated with an irrelevant control antibody. Each histogram represents 10,000 cells. The result shown is representative of several independent experiments.

hydrophobicity on the molecule. Both WT and DG clusterin showed a similar increase in *F*max when comparing the values at pH 7.5 to those at pH 6.0 (Figure 2B, Table 2). This implies that both showed, to a similar extent, the previously described substantial increase in exposure of hydrophobicity to solvent at mildly acidic pH that is associated with increased chaperone activity (*4*). The slightly higher exposed hydrophobicity of DG clusterin may explain its greater tendency to oligomerize in solution. It is well-known that clusterin aggregates in aqueous solution and at physiological pH exists as an equilibrium mixture of monomers, dimers, and higher aggregation states (*1*). When analyzed by size exclusion chromatography and compared with WT clusterin, at pH 7.5, DG clusterin showed a clear bias toward larger aggregation states (Figure 3, upper panel). At pH 6.0, WT clusterin showed the previously described shift toward lower order aggregation states (*4*). This shift was also evident for DG clusterin; however, even at this lower pH, a greater proportion of the molecules were in higher order aggregation states (compare upper and lower panels in Figure 3). In summary, deglycosylation of human clusterin had little effect on its overall secondary structural content (as judged by far-UV CD) or on the ability of mildly acidic pH to induce its dissociation toward lower order aggregation states but slightly increased the solvent-exposed hydrophobicity of the molecule and enhanced its overall tendency to form large aggregates in aqueous solution, regardless of the pH.

As expected, mildly acidic pH enhanced the binding of WT clusterin to all ligands tested (*4*); DG clusterin also showed a similar enhancement of binding at lower pH (Figure 4). With the exception of GST, DG clusterin bound to all ligands tested in ELISA with higher affinity than that of WT clusterin (Table 3) and in the cases of native IgG (at pH 7.5), heat-stressed lysozyme and reductively stressed BSA (at both pH 6.0 and 7.5) also bound to a higher level (Figure 4). Thus, the removal of sugars from clusterin increased its ability to bind to a variety of stressed and unstressed ligands at both pH 6.0 and 7.5. This may reflect the slightly greater exposed hydrophobicity of DG clusterin, which may contribute to ligand binding sites. Alternatively, or in addition, the sugars may to some extent sterically hinder ligand binding, and their removal provides ligands with enhanced access to binding sites. The observation that the affinities of WT and DG clusterin for native GST were similar at both pH 6.0 and 7.5 suggests that the binding site(s) for GST may be discrete from those for the other ligands tested. This interpretation is supported by earlier results indicating that clusterin has multiple ligand binding sites (*5*). The SPR data did not reveal a significant difference in overall affinity but showed faster on- and off-rates for DG clusterin (Table 4), suggesting that the carbohydrate may stabilize the binding to megalin by influencing the steric accessibility of the clusterin binding site(s). The K_d for the binding of clusterin to megalin has been previously estimated by ELISA in which megalin was adsorbed to the solid phase, giving values of 2.8 and 3.8 nM for porcine and human megalin, respectively (*28*). However, in the same study, a homologous ligand competition assay was used to estimate the K_d for the binding of clusterin to human megalin as 14.2 nM (*28*). Our SPR-determined estimate of K_d for the same binding event ($\sim$150 nM) was an order of magnitude greater. Collectively, these results suggest that the physical context of megalin (i.e., if and how it is immobilized to a solid phase, or in solution) can have large effects on its apparent affinity for clusterin.

Clusterin is known to form soluble high molecular weight complexes with partly unfolded proteins under stress conditions (*2*). We initially hypothesized that the very substantial amount of sugar conjugated to WT clusterin might be important in keeping these large complexes in solution and, therefore, that deglycosylation might reduce the ability of clusterin to inhibit protein precipitation. However, using citrate synthase as a heat-sensitive model, this was found not to be the case. In fact, at pH 7.5 (clusterin/CS = 0.65: 1.0), DG clusterin was slightly more effective at inhibiting heat-induced precipitation of CS than WT clusterin (Figure 6, upper panel). As expected (*4*), WT clusterin was a more efficient chaperone at pH 6.0 than at pH 7.5 (compare uper and lower panels in Figure 6). DG clusterin inhibited CS precipitation to a similar extent at pH 6.0 and 7.5. Results discussed above indicate that DG clusterin binds more strongly than WT clusterin to a broad range of ligands, including heat-stressed lysozyme and reductively stressed BSA. Thus, it is very likely that in solution, DG clusterin binds more strongly than WT clusterin to unfolding CS. At pH 7.5, this enhanced binding may explain the slightly greater efficiency with which DG clusterin inhibits CS precipitation. These results also imply that under these conditions, the overall hydrophilicity of the sugar-stripped clusterin polypeptide is sufficient to maintain the solubility of the clusterin−CS complexes. At pH 6.0, the efficiency of WT clusterin appears to approximately equal that of DG clusterin. Both WT and DG clusterin show a shift toward lower order aggregates at pH 6.0, which have been implicated in the chaperone action (*4*). It is not known why the efficiency of the chaperone action of DG clusterin did not increase at pH 6.0, but this might relate to the fact that at the lower pH, the clusterin polypeptide is close to its isoelectric point (predicted to be about 5.8, Swiss-Prot data base) and will, therefore, have a lower overall solubility.

Although the removal of sugars from clusterin did not have a large effect on its net binding to megalin, a number of other cell surface receptors have been implicated in binding clusterin (*24*, *29*). It is possible that clusterin may interact via its conjugated sugars with lectin-type cell surface receptors. As a first step toward investigating this possibility,

we compared the binding of WT and DG clusterin to the surface of HepG2 liver cells in the presence and absence of monomeric galactose (a potential competitive inhibitor of sugar−lectin interactions). Liver cells are known to express a broad variety of cell surface receptors, including those specific for carbohydrates (*30*). Although galactose had little effect on the binding of DG clusterin to HepG2 cells, it significantly inhibited the binding of WT clusterin to the same cell type (Figure 7). Although we have not identified the specific receptor(s) involved, this result suggests that at least part of the binding of WT clusterin to liver cells is mediated by one or more carbohydrate-specific receptors. Thus, one *in vivo* function for the sugars conjugated to clusterin may be to direct it for binding and uptake by specific lectin-type receptors. This is consistent with the recently proposed hypothesis that clusterin and other abundant extracellular chaperones may act *in vivo* to bind to and mediate the clearance of "damaged" (misfolded) proteins from extracellular fluids via receptor-mediated endocytosis (*7*).

In summary, the removal of conjugated sugars from WT clusterin had little effect on its overall secondary structure content but exposed slightly more hydrophobicity to solution and enhanced the propensity of the molecule to aggregate in solution. These changes were associated with increased binding to a variety of ligands but did not substantially impact the ability of clusterin to inhibit heat-induced precipitation of CS. BiaCore analyses comparing WT and DG clusterin indicate that as expected, the binding of clusterin to megalin is mediated at least primarily via interactions with the clusterin polypeptide. In contrast, at least part of the binding of WT clusterin to HepG2 liver cells is inhibitable by a monomeric sugar, suggesting that it may involve interaction with a lectin-type receptor. These findings provide insights that are likely to be useful in future studies of clusterin structure and function. Bulk expression of fully processed, glycosylated clusterin in mammalian cells is difficult, often producing inappropriately disulfide-bonded high molecular weight aggregates (unpublished results). This has previously severely hampered site-directed mutagenesis studies aimed at identifying those regions of the molecule important in its chaperone action. The current results identify for the first time that it may be possible in the future to study the structure and chaperone function of clusterin using recombinant protein (lacking sugars) conveniently bulk-expressed in bacteria.

ACKNOWLEDGMENT

We thank Wollongong Hospital for kindly donating human blood for use in this study.

REFERENCES

1. Humphreys, D., Carver, J. A., Easterbrook-Smith, S. B., and Wilson, M. R. (1999) Clusterin has chaperone-like activity similar to that of small heat-shock proteins, *J. Biol. Chem. 274*, 6875−6881.
2. Poon, S., Rybchyn, M. S., Easterbrook-Smith, S. B., Carver, J. A., and Wilson, M. R. (2000) Clusterin is an ATP-independent chaperone with very broad substrate specificity that stabilizes stressed proteins in a folding-competent state, *Biochemistry 39*, 15953−15960.
3. Poon, S., Treweek, T. M., Wilson, M. R., Easterbrook-Smith, S. B., and Carver, J. A. (2002) Clusterin, a unique extracellular chaperone, specifically interacts with slowly aggregating proteins on their off-folding pathway, *FEBS Lett. 513*, 259−266.
4. Poon, S., Rybchyn, M. S., Easterbrook-Smith, S. B., Carver, J. A., Pankhurst, G. J., and Wilson, M. R. (2002) Mildly acidic pH activates the extracellular molecular chaperone clusterin, *J. Biol. Chem. 277*, 39532−39540.
5. Lakins, J. N., Poon, S., Easterbrook-Smith, S. B., Carver, J. A., Tenniswood, M. P., and Wilson, M. R. (2002) Evidence that clusterin has discrete chaperone and ligand binding sites, *Biochemistry 41*, 282−291.
6. Yerbury, J., Easterbrook-Smith, S. B., Rybchyn, M. S., Henriques, C., and Wilson, M. R. (2005) The acute phase protein haptoglobin is a mammalian extracellular chaperone with an action similar to clusterin, *Biochemistry 44*, 10914−10925.
7. Yerbury, J., Wyatt, A., Stewart, E., and Wilson, M. R. (2005) Quality control of protein folding in extracellular space, *EMBO Rep. 6*, 1131−1136.
8. Rosenberg, M. E., Girton, R., Finkel, D., Chmielewski, D., Barrie, A., Witte, D. P., Zhu, G., Bissler, J. J., Harmony, J. A. K., and Aronow, B. J. (2002) Apolipoprotein J/clusterin prevents a progressive glomerulopathy of aging, *Mol. Cell. Biol. 22*, 1893−1902.
9. Jenne, D. E., and Tschopp, J. (1992) Clusterin: The intriguing guises of a widely expressed glycoprotein, *Trends Biochem. Sci. 17*, 154−159.
10. Kapron, J. T., Hilliard, G. M., Lakins, J. N., Tenniswood, M. P. R., West, K. A., Carr, S. A., and Crabb, J. W. (1997) Identification and characterization of glycosylation sites in human serum clusterin, *Protein Sci. 6*, 2120−2133.
11. Wilson, M. R., Roeth, P. J., and Easterbrook-Smith, S. B. (1991) Clusterin enhances the formation of insoluble immune complexes, *Biochem. Biophys. Res. Commun. 177*, 985−990.
12. Wilson, M. R., and Easterbrook-Smith, S. B. (1992) Clusterin binds by a multivalent mechanism to the Fc and Fab regions of IgG, *Biochim. Biophys. Acta 1159*, 319−326.
13. Heuer, K. H., Mackay, J. P., Podzebenko, P., Bains, N. P., Weiss, A. S., King, G. F., and Easterbrook-Smith, S. B. (1996) Development of a sensitive peptide-based immunoassay: application to detection of the Jun and Fos oncoproteins, *Biochemistry 35*, 9069−9075.
14. Wilson, M. R., and Easterbrook-Smith, S. B. (1993) Enzyme complex amplification: a signal amplification method for use in enzyme immunoassays, *Anal. Biochem. 209*, 183−187.
15. Humphreys, D., Hochgrebe, T. T., Easterbrook-Smith, S. B., Tenniswood, M. P., and Wilson, M. R. (1997) Effects of clusterin overexpression on TNFα- and TBFβ-mediated death of L929 cells, *Biochemistry 36*, 15233−15243.
16. Johnson, W. C. (1999) Analyzing protein circular dichroism spectra for accurate secondary structures, *Proteins: Struct., Funct., Genet. 35*, 307−312.
17. Provencher, S. W., and Glochner, J. (1981) Estimation of protein secondary structure from circular dichroism, *Biochemistry 20*, 33−37.
18. Wilson, M. R., and Easterbrook-Smith, S. B. (2000) Clusterin is a secreted mammalian chaperone, *Trends Biochem. Sci. 25*, 95−98.
19. Moestrup, S. K., Nielsen, S., Andreasen, P., Jorgensen, K. E., Nykjaer, A., Roigaard, H., Gliemann, J., and Christensen, E. I. (1993) Epithelial glycoprotein-330 mediates endocytosis of plasminogen activator-plasminogen activator inhibitor type-1 complexes, *J. Biol. Chem. 5*, 16564−16570.
20. Chu, F. K. (1986) Requirements of cleavage of high mannose oligosaccharides in glycoproteins by peptide N-glycosidase F, *J. Biol. Chem. 261*, 172−177.
21. Hames, B. (1994) One-Dimensional Polyacrylamide Gel Electrophoresis, in *Gel Electrophoresis of Proteins: A Practical Approach* (Rickwood, D., and Hames, B., Eds.) pp 1−139, IRL Press, Oxford, U.K.
22. Hochgrebe, T., Pankhurst, G. J., Wilce, J., and Easterbrook-Smith, S. B. (2000) pH-dependent changes in the in vitro ligand-binding properties and structure of human clusterin, *Biochemistry 39*, 1411−1419.
23. Carver, J. A., Rekas, A., Thorn, D. C., and Wilson, M. R. (2003) Small heat-shock proteins and clusterin: intra- and extracellular molecular chaperones with a common mechanism of action and function, *IUBMB Life 55*, 661−668.
24. Bartl, M. M., Luckenbach, T., Bergner, O., Ullrich, O., and Koch-Brandt, C. (2001) Multiple receptors mediate apoJ-dependent

clearance of cellular debris into nonprofessional phagocytes, *Exp. Cell Res. 271*, 130−141.
25. de Silva, H. V., Harmony, J. A. K., Stuart, W. D., Gil, C. M., and Robbins, J. (1990) Apolipoprotein J: structure and tissue distribution, *Biochemistry 29*, 5380−5389.
26. Kirszbaum, L., Sharpe, J. A., Murphy, B., d'Apice, A. J. F., Classon, B., Hudson, P., and Walker, I. D. (1989) Molecular cloning and characterization of the novel, human complement-associated protein, SP-40,40: a link between the complement and reproductive systems, *EMBO J. 8*, 711−718.
27. Matthews, K. W., Mueller-Ortiz, S. L., and Wetsel, R. A. (2004) Carboxypeptidase N: a pleiotropic regulator of inflammation, *Mol. Immunol. 40*, 785−793.
28. Kounnas, M. Z., Loukinova, E. B., Stefansson, S., Harmony, J. A. K., Brewer, B. H., Strickland, D. K., and Argraves, W. S. (1995) Identification of glycoprotein 330 as an endocytic receptor for apolipoprotein J/clusterin, *J. Biol. Chem. 270*, 13070−13075.
29. Bajari, T. M., Strasser, V., Nimpf, J., and Schneider, W. J. (2003) A model for modulation of leptin activity by association with clusterin. *FASEB J. 17*, 1505−7.
30. Ashwell, G., and Harford, J. (1982) Carbohydrate-specific receptors of the liver, *Annu. Rev. Biochem. 51*, 534−554.

BI062082V